electronics

MDPI

Article

Infinity Shell Shaped MIMO Antenna Array for mm-Wave 5G Applications

Mian Muhammad Kamal [1,*], Shouyi Yang [1], Xin-cheng Ren [2], Ahsan Altaf [3], Saad Hassan Kiani [4], Muhammad Rizwan Anjum [5], Amjad Iqbal [6], Muhammad Asif [4] and Sohail Imran Saeed [7,*]

1 School of Information Engineering, Zhengzhou University, Zhengzhou 450001, China; iesyyang@zzu.edu.cn
2 School of Physics and Electronic Information, Yanan University, Shaanxi 761000, China; xchren@yau.edu.cn
3 Electrical Engineering Department, Istanbul Medipol University, 34083 Istanbul, Turkey; aaltaf@st.medipol.edu.tr
4 Electrical Engineering Department, City University of Science and Information Technology, Peshawar 25000, Pakistan; saad.kiani@cusit.edu.pk (S.H.K.); masifee@cusit.edu.pk (M.A.)
5 Department of Electronic Engineering, The Islamia University of Bahawalpur, Bahawalpur 63100, Pakistan; engr.rizwan@iub.edu.pk
6 Faculty of Engineering, Multimedia University, Cyberjaya 63100, Malaysia; aiqbal@ieee.org
7 Electrical Engineering Department, Iqra National University, Peshawar 25000, Pakistan
* Correspondence: mmkamal@gs.zzu.edu.cn (M.M.K.); sohail.imran@inu.edu.pk (S.I.S.)

Abstract: In this paper, a novel single layer Multiple Input–Multiple Output (MIMO) antenna for Fifth-Generation (5G) 28 GHz frequency band applications is proposed and investigated. The proposed MIMO antenna operates in the Ka-band, which is the most desirable frequency band for 5G mm-wave communication. The dielectric material is a Rogers-5880 with a relative permittivity, thickness and loss tangent of 2.2, 0.787 mm and 0.0009, respectively, in the proposed antenna design. The proposed MIMO configuration antenna element consists of triplet circular shaped rings surrounded by an infinity-shaped shell. The simulated gain achieved by the proposed design is 6.1 dBi, while the measured gain is 5.5 dBi. Furthermore, the measured and simulated antenna efficiency is 90% and 92%, respectively. One of the MIMO performance metrics—i.e., the Envelope Correlation Coefficient (ECC)—is also analyzed and found to be less than 0.16 for the entire operating bandwidth. The proposed MIMO design operates efficiently with a low ECC, better efficiency and a satisfactory gain, showing that the proposed design is a potential candidate for mm-wave communication.

Keywords: 5G antenna; shell; gain; 5G; devices; directivity; bandwidth

Citation: Kamal, M.M.; Yang, S.; Ren, X.-c.; Altaf, A.; Kiani, S.H.; Anjum, M.R.; Iqbal, A.; Asif, M.; Saeed, S.I. Infinity Shell Shaped MIMO Antenna Array for mm-Wave 5G Applications. *Electronics* **2021**, *10*, 165. https://doi.org/10.3390/electronics10020165

Received: 23 November 2020
Accepted: 6 January 2021
Published: 13 January 2021

1. Introduction

Fifth Generation (5G) communication has now become the most discussed technology. The reason for the great attraction of 5G is the continuously progressing demand for higher data rates and bandwidth, which is not possible to fulfill with the current standards below the 5G technology [1,2]. The limited bandwidth availability in the microwave region and highly busy portion of the spectrum have forced a move towards a new spectrum range which can offer data rates in the range of multi-gigabits per second (Gbps) [3]. 5G is currently divided into sub-6 GHz and mm-wave regions to achieve the required data rates and bandwidth targets [4–7]. In this portion of the spectrum, the 28 GHz band has attracted a great deal of attention from the research community due to the low atmospheric attenuation, which is one of the most important and non-ignorable issues in mm-wave communication [8,9]. Because these attenuations make the signal weak when traveling from the transmitter to the receiver side, a low-quality and weak strength signal is received by the user [10,11]. A high gain antenna with a Multiple Input Multiple Output (MIMO) configuration can resolve these issues and improve the user communication experience by using the multi-path property [12–15]. In the literature, several antennas have been

reported for mm-wave applications. A study [16] reports a 5G antenna with a MIMO configuration possessing a 23–40 GHz wide response. The area of the proposed design is noted to be 80 × 80 mm^2. Although a huge bandwidth is achieved by the proposed MIMO design, the size of it is observed to be quite large. Similarly, a circular, polarized MIMO antenna with four ports is presented in [17]. An antenna element is placed within a center of a large number of parasitic elements to improve the radiation characteristics; however, the complexity of the proposed MIMO design is increased due to the use of parasitic elements. In Reference [18], the authors present a single antenna element with an overall size of 10 × 6 mm^2 with a 6.59 dB maximum gain. Although the gain achieved by the antenna element is sufficient, the implementations of electromagnetic band-gap structures (EBG) make the coupling issues severe and the fabrication task difficult. Likewise, array antenna operation at two frequency bands—i.e., 28 GHz and 38 GHz—is proposed in [19]. The high gain of the reported antenna makes this option attractive, but it lacks the MIMO property. An 8 × 8 MIMO configuration with a total volume of 31.2 × 31.2 × 1.57 mm^3 is proposed in [20], giving a resonance at 25.2 GHz with a 8.7 dB maximum gain, while large numbers of back and side lobes are observed in the proposed antenna radiation response. In Reference [21], an antenna for 4G and 5G applications is presented, giving a resonance of 28 GHz with a total antenna size of 75 × 85 mm^2. The gain yielded at the mm-wave band is 5.13 dB, while large numbers of back and side lobes are found in the radiation response, which make the proposed antenna undesirable for mm-wave communication. Similarly, a mm-wave antenna design with a T-shaped structure covering the frequency band approximately from 25.1 GHz to 37.5 GHz is proposed in [22], while a four-element antenna with an area of 30 × 35 mm^2 and a peak gain of 8.3 dB and a MIMO antenna working in the 28 GHz frequency band are proposed in [23,24], respectively.

With the announcement of 5G sub-6 GHz and mm-wave potential bands, the mm-wave 28 GHz band has been seen as a potential candidate for future mm-wave smartphones. Several studies [25–28] have reported reserved space for mm-wave antennas, and some have included mm-wave designs. In Reference [26], a multi-band four-port antenna system is reported with an overall length and width of 158 × 78 mm^2 with a gain of 5.1 dB at 28 GHz frequency. The mm-wave antenna generated three different resonances of 28 GHz, 37 GHz and 39 GHz. The four antennas are placed on the central edges of the board, but their individual dimensions limit them to a maximum of four elements. In Reference [27], a novel T slot four-element antenna system consisting of two element-feed networks is presented, with each resonating at two distinct bands: one below sub-6 GHz and the other in the mm-wave band from 24 GHz to 29 GHz with a peak gain of 5 dB at 28 GHz. Although the study reported stable radiation patterns and performance parameters, the ground plane assembly and larger dimensions of radiating elements prevent the structure from being used with higher numbers of elements. An eight-port tapered slot antenna system with overall dimensions of 104 × 104 × 0.501 mm^3 is reported in [28]. The antenna exhibited dual-band frequency response on a lower frequency band of 2.45 GHz and higher mm-wave mode of 28 GHz, providing an isolation level of 16 dB among two radiating elements and an efficiency of 80%. The reported multi-band antenna system with a tapered slot increases the overall complexity of the system. In these studies, it is observed that mm-wave resonating structures are complex and large in dimension. As 5G mainly focuses on high data rates with less latency as compared to 4G systems, the mm-wave currently has a huge bandwidth to be occupied and to be used since the sub-6 GHz spectrum is already congested. From the reported literature, single element structures have been observed, as well as those in linear array forms without MIMO assemblies. This work focuses on developing an MIMO antenna with fewer coupling phenomena for 28 GHz mm-wave applications. Therefore, the development of novel-shaped antenna with a circular ring-shaped radiating structure for the mm-wave applications with high isolation without the addition of a defected ground slot (DGS), tapered slot or electromagnetic band gap (EBG) structures is presented. The proposed shape is transformed into an MIMO configuration of four elements, and good impedance bandwidth and gain is achieved. The proposed

structure can easily be embedded in smart phones as it provides and satisfies pattern diversity and all essential MIMO characteristics.

2. Antenna Design

The proposed antenna design was printed on a 0.787 mm thick Rogers 5880 substrate with a relative permittivity of 2.2 and loss tangent of 0.0009. The front view of the single element is shown in Figure 1. The proposed design comprised five ring structures fused in such a way that a modified novel spiral shape was formed. The dimensions of proposed element were as follows: Circle 1 = 4 mm, Circle 2 = 1.5 mm and feed length = 10 mm with a feed width of 0.76 mm. The width of the circular slots was kept at 0.4 mm, and the distance between larger and smaller rings was also kept 0.4 mm. The length and width of the substrate was an LS of 14 mm and WS of 14 mm, while the length of the ground plane was kept at 7 mm only. The ground plane was incorporated with a half circle with an outer radius of 3 mm and inner radius of 2.6 mm, respectively.

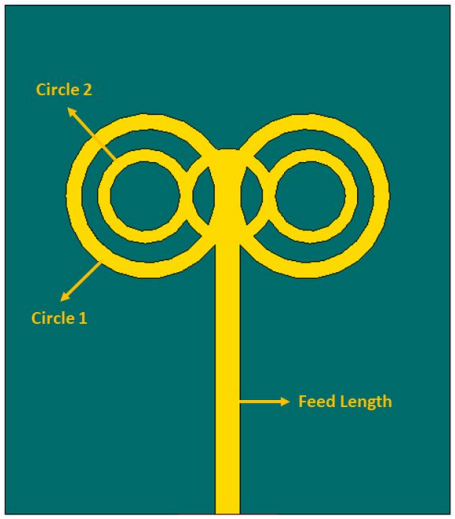

Figure 1. Proposed single-element antenna.

MIMO Configuration

The proposed structure was transformed into a four-port MIMO array with an overall length and width of 30 mm × 30 mm as shown in Figure 2. The MIMO assembly was arranged in such a way that the radiating elements were at a 90° distance from each other.

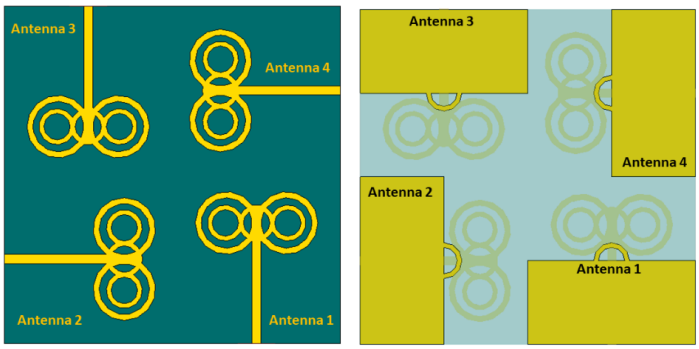

(**a**) (**b**)

Figure 2. Multiple Input–Multiple Output (MIM) configuration. (**a**) View of the front; (**b**) view of the back.

Such a MIMO configuration has been found useful as it offers fewer coupling effects and provides much better spatial and pattern diversity. Copper with a very stable con-

ductivity of 5.8 × 10^7 S/m was used for the radiating element. Due to the very stable conductivity of copper, its effect on the impedance matching was very low. The proposed design was modeled in Computer Simulation Technology CST (2017) under a higher meshing environment.

3. Results and Discussion

The proposed MIMO antenna was designed in CST microwave studio 2017 and fabricated using an LPKF (Leiterplatten–Kopierfrasen) machine. Figure 3 shows the proposed design fabricated model.

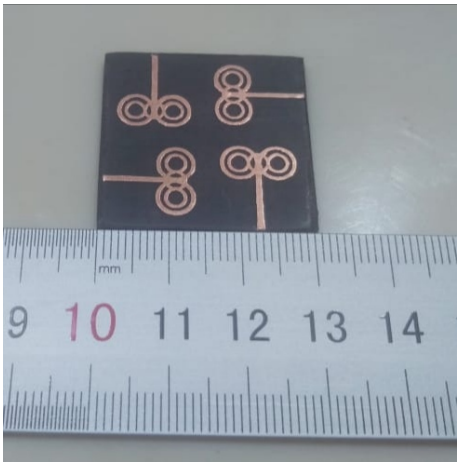

Figure 3. Fabricated prototype of MIMO array.

3.1. S Parameter Analysis

The S-parameter response is discussed in this section. The single-element reflection co-efficient response was tuned at 28 GHz with an impedance bandwidth of 2 GHz, as shown in Figure 4. In the MIMO configuration, the reflection co-efficient responses of Antenna 1 and Antenna 2 were slightly shifted but sufficiently covered the required bandwidth. Due to the perpendicular placement of radiating elements, the isolation of MIMO ports was found to be better than −29 dB. The simulated S-parameter response is shown in Figure 5a,b, while measured results are shown in Figure 5c,d. The measured coefficient results are slightly shifted, which can be attributed to human and measuring environment error. The measured isolation levels of the antenna were also found to be better than −29 dB levels, confirming the performance characteristics of the proposed structure.

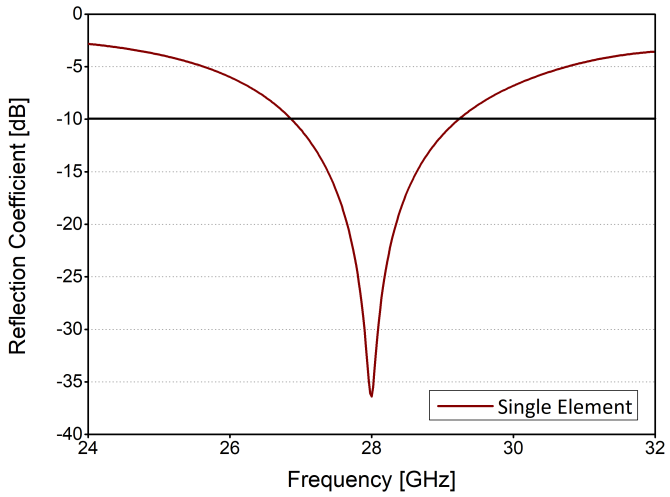

Figure 4. Simulated S-parameter of the single element.

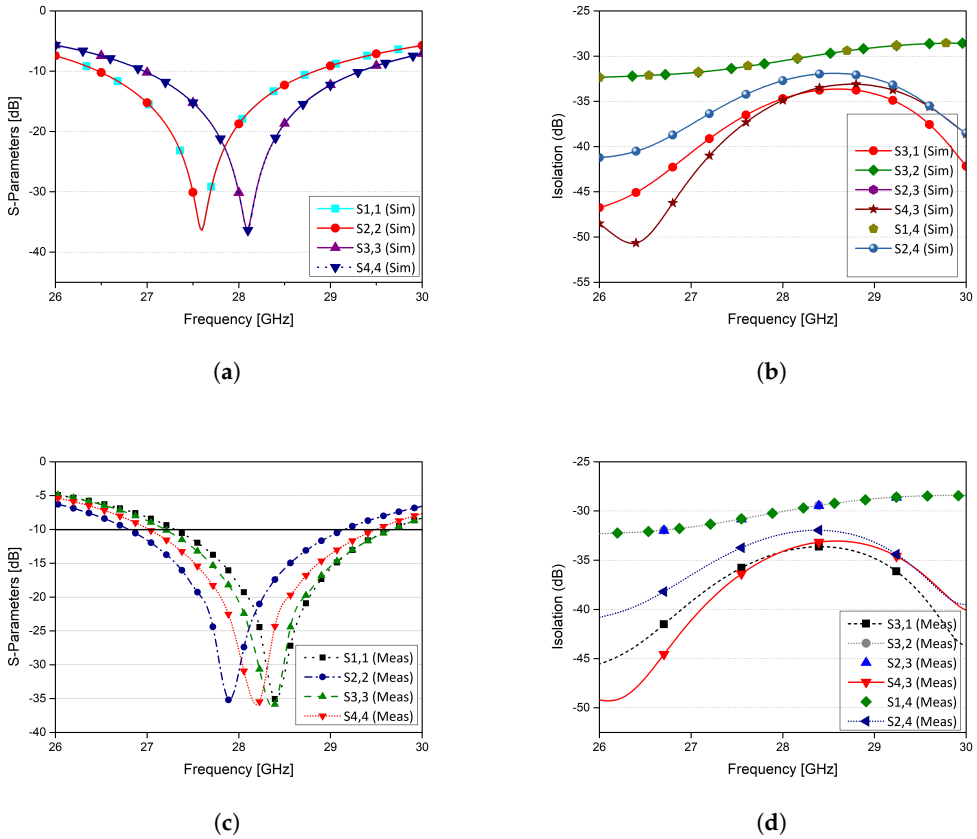

Figure 5. (**a**) Reflection coefficient of the proposed MIMO configuration, (**b**) simulated port isolation, (**c**) measured reflection coefficient of the proposed MIMO configuration, (**d**) measured port isolation.

3.2. Radiation Pattern

The simulated and measured radiation patterns were taken at a central frequency of 28 GHz on two principal planes, which were E and H planes, or at $\phi = 0^\circ$ and $\phi = 90^\circ$ as shown in Figure 6. The main lobe direction of antenna 1 in $\phi = 0^\circ$ was between 90° and 150°, while at $\phi = 90^\circ$, the main lobe was between 60° and 90°. Similarly, antenna 3 was the mirror image of antenna 1, and the radiation patterns of antenna 3 showed the main lobe between 210° and 270°; at $\phi = 90^\circ$, the main lobe was between 240° and 300°. Regarding the radiation characteristics of antenna 2 and antenna 4, the main lobe was found to be in a reverse order to that of antenna 1 and antenna 3. This can be attributed to the perpendicular MIMO assembly of radiating elements, thus providing unique pattern diversity characteristics that are helpful for mitigating the multipath effect for communication systems. The variations in the simulated and measured radiation patterns can be attributed to the presence of attenuation and cable losses with probability of error in measuring the far-field setup. Although slight variation exists, the proposed MIMO structure gives a good impression of the simulated and measured radiation patterns. The antenna's efficiency is given in Figure 7, which clearly shows that proposed structure is highly efficient throughout the band of interest. Figure 8 shows the 3D radiation patterns of the proposed MIMO antenna system. The 3D figures shows that the proposed antenna system provides pattern diversity from each port.

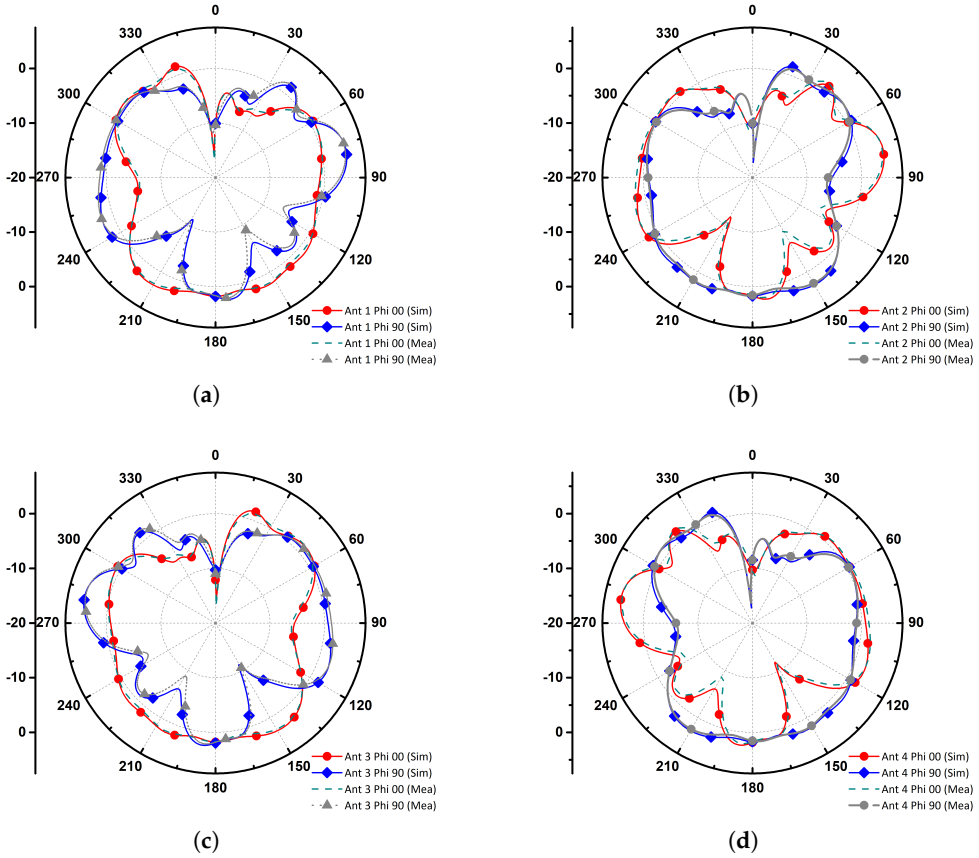

Figure 6. Simulated and measured radiation patterns: (**a**) AE-1 (**b**) AE-2 (**c**) AE-3 (**d**) AE-4. The polar coordinates show degrees, the y-axis is plotted in dBi.

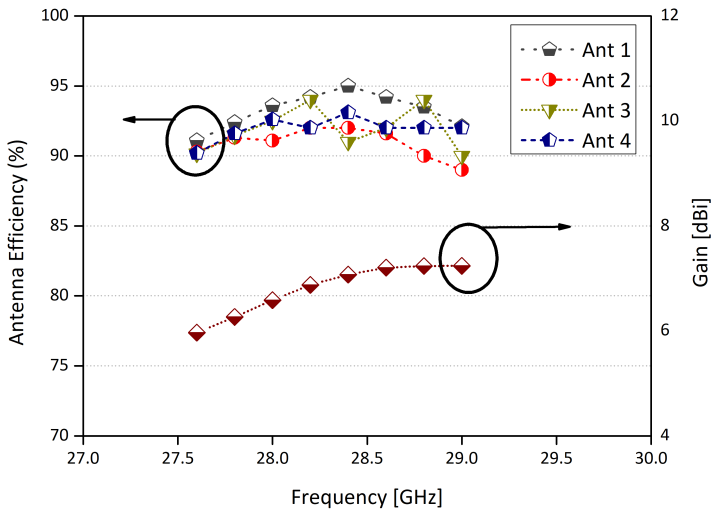

Figure 7. Antenna Efficiency and Simulated Gain of MIMO configuration.

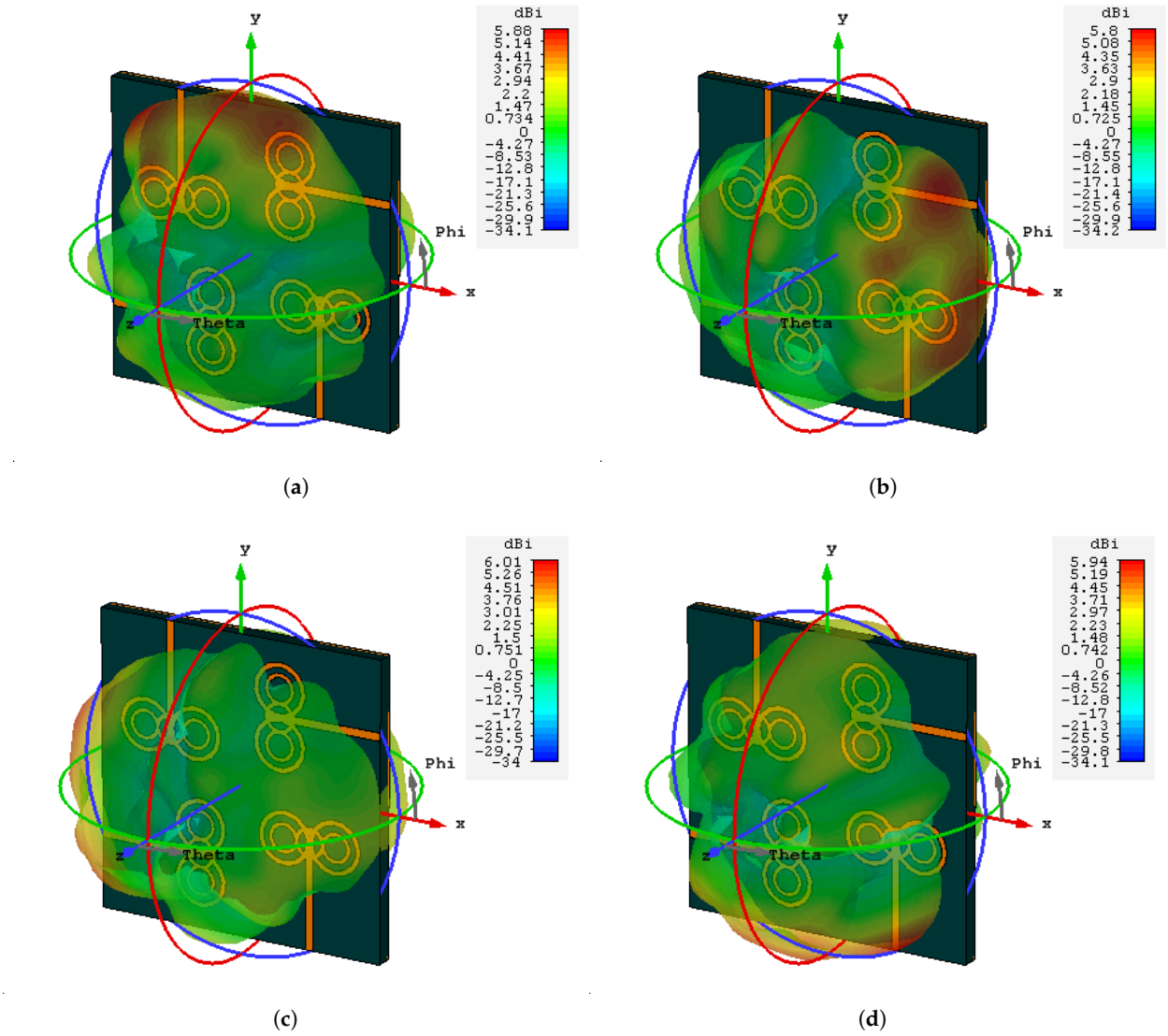

Figure 8. Simulated and measured radiation patterns (**a**) AE-1 (**b**) AE-2 (**c**) AE-3 (**d**) AE-4.

3.3. Surface Current Distributions

Figure 9 shows the distribution of the surface current for the proposed design operating at the 28 GHz band of interest for each antenna element, respectively. From the distribution of the surface current, it can be seen that the intensity of the current is high around the connected circle-shaped rings, showing that the contribution of these circular-shaped rings is more significant in the mm-wave band. Moreover, the level of the coupling among the elements is quite ignorable according to the distribution pattern of the current, which is achieved by the assembly of the elements with a shift of 90° per element.

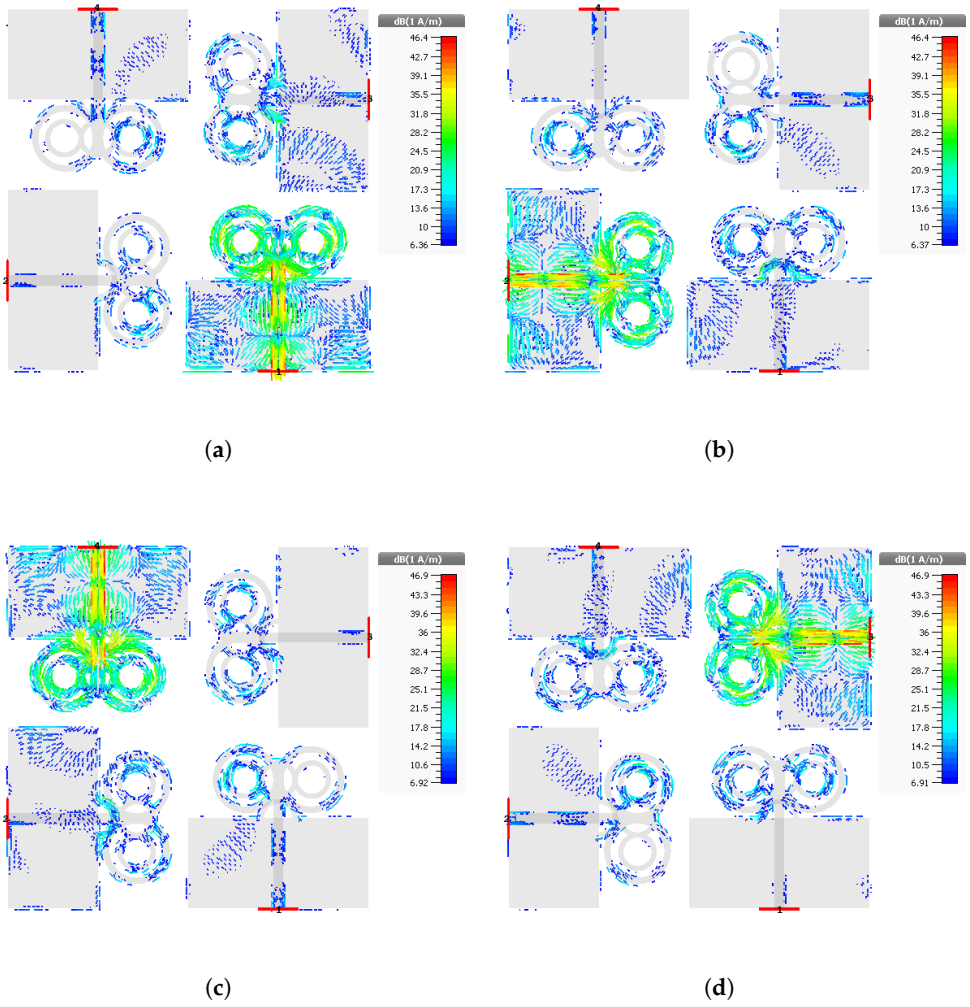

(**a**) (**b**)

(**c**) (**d**)

Figure 9. Distribution pattern of current at 28 GHz for (**a**) antenna 1, (**b**) antenna 2, (**c**) antenna 3, (**d**) antenna 4.

4. Mimo Parameters

4.1. Envelope Correlation Coefficient

To check the level of the coupling among elements of the proposed MIMO antenna, the envelope correlation coefficient (ECC) is evaluated. The S-parameter method is utilized to evaluate the response of the ECC [29]. A low value of the ECC—i.e., below 0.16—is observed in Figure 10 across the desired band, showing that the level of interference is low among the elements.

$$ECC = \frac{|\iint_{4\pi}(\vec{B}_i(\theta,\phi)) \times (\vec{B}_j(\theta,\phi))\, d\Omega|^2}{\iint_{4\pi}|(\vec{B}_i(\theta,\phi))|^2\, d\Omega \iint_{4\pi}|(\vec{B}_j(\theta,\phi))|^2\, d\Omega} \quad (1)$$

where $\vec{B}_i(\theta,\phi)$ denotes the 3D radiation pattern upon the excitation of the i^{th} antenna and $\vec{B}_j(\theta,\phi)$ denotes the 3D radiation pattern upon the excitation of the j^{th} antenna. Ω is the solid angle.

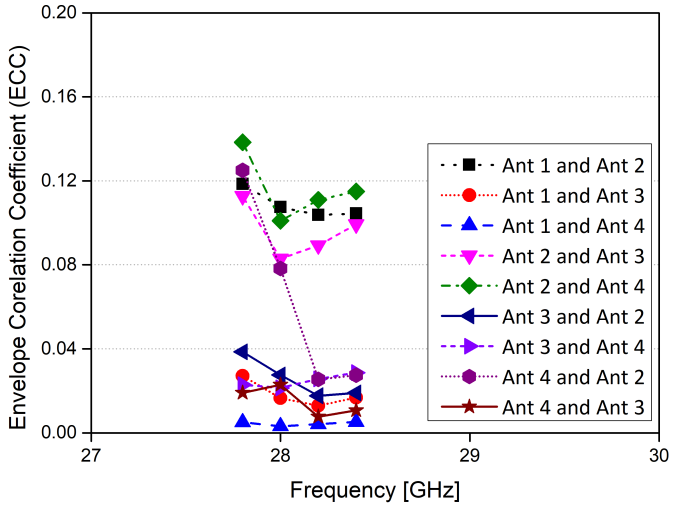

Figure 10. Envelope correlation coefficient for the MIMO antenna.

4.2. Mean Effective Gain (MEG)

The mean effective gain (MEG) is an important MIMO performance parameter which evaluates power imbalances in the MIMO system over a propagation environment. To fulfill the balance power standard and for optimal diversity performance with a good channel characteristic, the alteration of the MEGs of any two antennas in the MIMO system should be less than 3 dB. The calculated MEG value of the proposed MIMO antenna is shown in Table 1 and is calculated through the standard equation presented in [5].

$$MEG = \int_{-\pi}^{\pi}\int_{0}^{\pi}[\frac{r}{r+1}G_{\theta}(\theta,\phi)P_{\theta}(\theta,\phi) + \frac{1}{1+r}G_{\phi}(\theta,\phi)P_{\phi}(\theta,\phi)]sin\theta d\theta d\phi \quad (2)$$

where $G_{\phi}(\theta,\phi)$ and $P_{\theta}(\theta,\phi)$ are angle of arrival and r is the cross polar ratio which can be expressed as Equation (3).

$$r = 10log_{10}(\frac{P_{vpa}}{P_{hpa}}) \quad (3)$$

where the powers received by the vertically polarized antenna and horizontally polarized antenna are represented as P_{vpa} and P_{hpa}, respectively.

Table 1. Calculated mean effective gain (MEG) values of the MIMO antenna.

Frequency (GHz)	MEG1 (dB)	MEG2 (dB)	MEG3 (dB)	MEG4 (dB)
28	−4.1	−3.9	−3.2	−3.1
28.5	−3.09	−2.87	−3.5	−3.4
29	−2.9	−3.02	−2.8	−3.4

Table 2 provides published work comparison with proposed four port MIMO structure.

Table 2. Literature Comparison with the proposed MIMO antenna.

Ref.	Ports	Size of Antenna in mm (LxW)	Isolation (dB)	Eff. %	Gain (dBi)	ECC
[4]	6	136 × 68	−10	50	3.9	<0.3
[5]	8	150 × 75	−12.5	70	4.9	<0.15
[30]	4	55 × 110	−28.32	88.25	8.27	<0.047
[31]	3	130 × 80	−53	80	10.3	N/A
[32]	4	26.6 × 3.25	N/A	N/A	5.2	N/A
[29]	4	19.25 × 26	−25	86	5.72	<0.04
[33]	2	55 × 110	−27.3	N/A	9.49	<0.06
[34]	2	26 × 11	−25	98.6	5.7	<0.01
Proposed	4	30 × 30	<−29	92	6.1	<0.16

5. Conclusions

In this article, a novel infinity-shaped MIMO antenna is presented that resonates at 28 GHz in the mm-wave band for future 5G communication devices. The proposed MIMO antenna consists of four antenna elements which are arranged with a shift of 90°. Each antenna element radiating portion consists of four circle-shaped ring patches, which contribute mostly to achieve the operation in the desired frequency band. Furthermore, these four circle-shaped rings surround another circle located at the center; above the feed line in the case of each antenna element, respectively. The isolation achieved for the operating bandwidth is better than −29 dB, demonstrating low mutual coupling. Moreover, the peak gain and total efficiency obtained are 6.1 dBi and 92%, respectively, for the operating bandwidth of the proposed MIMO antenna. The lower value of ECC (<0.16), satisfactory efficiency and gain, good return loss and decent coherence between the simulated and measured results make the proposed design a competent candidate for future 5G-based mm-wave communication.

Author Contributions: Conceptualization, S.H.K. and M.M.K.; methodology, S.H.K., A.I. and A.A.; Software, S.H.K. and M.M.K.; Validation, A.I., S.I.S. and A.A.; Formal Analysis, A.A., S.I.S. and X.-c.R.; Investigation, S.H.K., M.R.A. and M.A.; Resources, A.I., M.A. and S.I.S.; Data Curation, S.H.K. and M.R.A.; Writing, original draft preparation, A.A. and X.R.; Writing, review and editing, S.Y. and M.M.K.; Project administration, X.-c.R., M.A. and S.Y.; Funding acquisition, X.-c.R. All authors have read and agreed to the published version of the manuscript.

Funding: This project was supported by the National Natural Science Foundation of China (61861043).

Data Availability Statement: No new data were created or analyzed in this study. Data sharing is not applicable to this article.

Conflicts of Interest: The authors declare no conflict of interest.

References

1. Varga, P.; Peto, J.; Franko, A.; Balla, D.; Haja, D.; Janky, F.; Soos, G.; Ficzere, D.; Maliosz, M.; Toka, L. 5g support for industrial iot applications–challenges, solutions, and research gaps. *Sensors* **2020**, *20*, 828. [CrossRef]
2. Hilt, A. Availability and Fade Margin Calculations for 5G Microwave and Millimeter-Wave Anyhaul Links. *Appl. Sci.* **2019**, *9*, 5240. [CrossRef]
3. Khalily, M.; Tafazolli, R.; Xiao, P.; Kishk, A.A. Broadband mm-wave microstrip array antenna with improved radiation characteristics for different 5G applications. *IEEE Trans. Antennas Propag.* **2018**, *66*, 4641–4647. [CrossRef]
4. Abdullah, M.; Kiani, S.H.; Abdulrazak, L.F.; Iqbal, A.; Bashir, M.; Khan, S.; Kim, S. High-performance multiple-input multiple-output antenna system for 5G mobile terminals. *Electronics* **2019**, *8*, 1090. [CrossRef]
5. Kiani, S.H.; Altaf, A.; Abdullah, M.; Muhammad, F.; Shoaib, N.; Anjum, M.R.; Damaševičius, R.; Blažauskas, T. Eight Element Side Edged Framed MIMO Antenna Array for Future 5G Smart Phones. *Micromachines* **2020**, *11*, 956. [CrossRef] [PubMed]
6. Pi, Z.; Khan, F. An introduction to millimeter-wave mobile broadband systems. *IEEE Commun. Mag.* **2011**, *49*, 101–107. [CrossRef]
7. Ullah, H.; Tahir, F.A. A Novel Snowflake Fractal Antenna for Dual-Beam Applications in 28 GHz Band. *IEEE Access* **2020**, *8*, 19873–19879. [CrossRef]

8. NetWorld2020 ETP. 5G: Challenges, Research Priorities, and Recommendations; Joint White Paper. September 2014. Available online: https://networld2020.eu/wp-content/uploads/2015/01/Joint-Whitepaper-V12-clean-after-consultation.pdf (accessed on 6 January 2021).
9. Shayea, I.; Rahman, T.A.; Azmi, M.H.; Islam, M.R. Real measurement study for rain rate and rain attenuation conducted over 26 GHz microwave 5G link system in Malaysia. *IEEE Access* **2018**, *6*, 19044–19064. [CrossRef]
10. Aliakbari, H.; Abdipour, A.; Costanzo, A.; Masotti, D.; Mirzavand, R.; Mousavi, P. Performance investigation of space diversity for a 28/38 GHz MIMO antenna (applicable to mm-wave mobile network). In Proceedings of the 2016 Fourth International Conference on Millimeter-Wave and Terahertz Technologies (MMWaTT), Tehran, Iran, 20–22 December 2016; pp. 41–44.
11. Sulyman, A.I.; Alwarafy, A.; MacCartney, G.R.; Rappaport, T.S.; Alsanie, A. Directional radio propagation path loss models for millimeter-wave wireless networks in the 28-, 60-, and 73-GHz bands. *IEEE Trans. Wirel. Commun.* **2016**, *15*, 6939–6947. [CrossRef]
12. Zhang, J.; Ge, X.; Li, Q.; Guizani, M.; Zhang, Y. 5G millimeter-wave antenna array: Design and challenges. *IEEE Wirel. Commun.* **2016**, *24*, 106–112. [CrossRef]
13. Wang, F.; Duan, Z.; Wang, X.; Zhou, Q.; Gong, Y. High Isolation Millimeter-Wave Wideband MIMO Antenna for 5G Communication. *Int. J. Antennas Propag.* **2019**, *2019*, 4283010. [CrossRef]
14. Guo, J.; Cui, L.; Li, C.; Sun, B. Side-edge frame printed eight-port dual-band antenna array for 5G smartphone applications. *IEEE Trans. Antennas Propag.* **2018**, *66*, 7412–7417. [CrossRef]
15. Yang, B.; Yu, Z.; Dong, Y.; Zhou, J.; Hong, W. Compact tapered slot antenna array for 5G millimeter-wave massive MIMO systems. *IEEE Trans. Antennas Propag.* **2017**, *65*, 6721–6727. [CrossRef]
16. Sehrai, D.A.; Abdullah, M.; Altaf, A.; Kiani, S.H.; Muhammad, F.; Tufail, M.; Irfan, M.; Glowacz, A.; Rahman, S. A Novel High Gain Wideband MIMO Antenna for 5G Millimeter Wave Applications. *Electronics* **2020**, *9*, 1031. [CrossRef]
17. Hussain, N.; Jeong, M.J.; Abbas, A.; Kim, N. Metasurface-based single-layer wideband circularly polarized MIMO antenna for 5G millimeter-wave systems. *IEEE Access* **2020**, *8*, 130293–130304. [CrossRef]
18. Khan, J.; Sehrai, D.A.; Khan, M.A.; Khan, H.A.; Ahmad, S.; Ali, A.; Arif, A.; Memon, A.A.; Khan, S. Design and Performance Comparison of Rotated Y-Shaped Antenna Using Different Metamaterial Surfaces for 5G Mobile Devices. *CMC-Comput. Mater. Contin.* **2019**, *60*, 409–420. [CrossRef]
19. Khan, J.; Sehrai, D.A.; Ali, U. Design of dual band 5G antenna array with SAR analysis for future mobile handsets. *J. Electr. Eng. Technol.* **2019**, *14*, 809–816. [CrossRef]
20. Shoaib, N.; Shoaib, S.; Khattak, R.Y.; Shoaib, I.; Chen, X.; Perwaiz, A. MIMO antennas for smart 5G devices. *IEEE Access* **2018**, *6*, 77014–77021. [CrossRef]
21. Iffat Naqvi, S.; Hussain, N.; Iqbal, A.; Rahman, M.; Forsat, M.; Mirjavadi, S.S.; Amin, Y. Integrated LTE and Millimeter-Wave 5G MIMO Antenna System for 4G/5G Wireless Terminals. *Sensors* **2020**, *20*, 3926. [CrossRef]
22. Jilani, S.F.; Alomainy, A. Millimetre-wave T-shaped antenna with defected ground structures for 5G wireless networks. In Proceedings of the 2016 Loughborough Antennas & Propagation Conference (LAPC), Loughborough, UK, 14–16 November 2016; pp. 1–3.
23. Khalid, M.; Iffat Naqvi, S.; Hussain, N.; Rahman, M.; Mirjavadi, S.S.; Khan, M.J.; Amin, Y. 4-Port MIMO antenna with defected ground structure for 5G millimeter wave applications. *Electronics* **2020**, *9*, 71. [CrossRef]
24. Wani, Z.; Abegaonkar, M.P.; Koul, S.K. A 28-GHz antenna for 5G MIMO applications. *Prog. Electromagn. Res.* **2018**, *78*, 73–79. [CrossRef]
25. Ojaroudi Parchin, N.; Jahanbakhsh Basherlou, H.; Alibakhshikenari, M.; Ojaroudi Parchin, Y.; Al-Yasir, Y.I.; Abd-Alhameed, R.A.; Limiti, E. Mobile-phone antenna array with diamond-ring slot elements for 5G massive MIMO systems. *Electronics* **2019**, *8*, 521. [CrossRef]
26. Al Abbas, E.; Ikram, M.; Mobashsher, A.T.; Abbosh, A. MIMO Antenna System for Multi-Band Millimeter-Wave 5G and Wideband 4G Mobile Communications. *IEEE Access* **2019**, *7*, 181916–181923. [CrossRef]
27. Naqvi, S.I.; Naqvi, A.H.; Arshad, F.; Riaz, M.A.; Azam, M.A.; Khan, M.S.; Amin, Y.; Loo, J.; Tenhunen, H. An integrated antenna system for 4G and millimeter-wave 5G future handheld devices. *IEEE Access* **2019**, *7*, 116555–116566. [CrossRef]
28. Ikram, M.; Nguyen-Trong, N.; Abbosh, A. Multiband MIMO microwave and millimeter antenna system employing dual-function tapered slot structure. *IEEE Trans. Antennas Propag.* **2019**, *67*, 5705–5710. [CrossRef]
29. Tu, D.T.T.; Thang, N.G.; Ngoc, N.T.; Phuong, N.T.B.; Van Yem, V. 28/38 GHz dual-band MIMO antenna with low mutual coupling using novel round patch EBG cell for 5G applications. In Proceedings of the 2017 International Conference on Advanced Technologies for Communications (ATC), Quy Nhon, Vietnam, 18–20 October 2017; pp. 64–69.
30. Marzouk, H.M.; Ahmed, M.I.; Shaalan, A.H.A.M. Novel dual-band 28/38 GHz MIMO antennas for 5G mobile applications. *Prog. Electromagn. Res.* **2019**, *93*, 103–117. [CrossRef]
31. Liu, Y.; Li, Y.; Ge, L.; Wang, J.; Ai, B. A Compact Hepta-Band Mode-Composite Antenna for Sub (6, 28, and 38) GHz Applications. *IEEE Trans. Antennas Propag.* **2020**, *68*, 2593–2602. [CrossRef]
32. Sunthari, P.M.; Veeramani, R. Multiband microstrip patch antenna for 5G wireless applications using MIMO techniques. In Proceedings of the 2017 First International Conference on Recent Advances in Aerospace Engineering (ICRAAE), Coimbatore, India, 3–4 March 2017; pp. 1–5.

33. Marzouk, H.; Ahmed, M.; Shaalan, A. A Novel Dual-band 28/38 GHz Slotted Microstip MIMO Antenna for 5G Mobile Applications. In Proceedings of the 2019 IEEE International Symposium on Antennas and Propagation and USNC-URSI Radio Science Meeting, Atlanta, GA, USA, 7–12 July 2019; pp. 607–608.
34. Ali, W.; Das, S.; Medkour, H.; Lakrit, S. Planar dual-band 27/39 GHz millimeter-wave MIMO antenna for 5G applications. *Microsyst. Technol.* **2020**, 1–10. [CrossRef]